

Commentary on “Total Hadronic Cross Section Data and the Froissart-Martin Bound”, by Fagundes, Menon and Silva

Martin M. Block¹ and Francis Halzen²

¹*Department of Physics and Astronomy, Northwestern University, Evanston, IL 60208*

²*Department of Physics, University of Wisconsin, Madison, WI 53706*

(Dated: October 21, 2018)

This Commentary on the paper, “Total Hadronic Cross Section Data and the Froissart-Martin Bound”, by Fagundes, Menon and Silva (Braz. J. Phys., Vol. 42 (2012); arXiv:1112.4704) was invited by the Editors of the Brazilian Journal of Physics to appear directly after the above authors printed version, in the same journal issue. We here challenge that paper’s conclusions that the Froissart bound was violated. We will show that this conclusion follows from a statistical methodology that we question, and will present compelling supplementary evidence that the latest ultra-high energy experimental pp cross section data are consistent with a $\ln^2 s$ behavior that satisfies the Froissart bound.

PACS numbers: 12.38.Qk, 13.85Hd, 13.85Lg, 13.85Tp

Introduction.—We have been invited by the Editors of the Brazilian Journal of Physics to write a back-to-back Commentary, to be published in the same printed journal, on “Total Hadronic Cross Section Data and the Froissart-Martin Bound”, by D. A. Fagundes, M. J. Menon and P. V. R. G. Silva, Braz. J. Phys., Vol. 42 (2012); arXiv:1112.4704, hereafter referred to as FMS [1]. We wish to challenge their conclusion that the original Froissart bound [2] is violated, i.e., their statement that the total pp ($\bar{p}p$) section rises more rapidly with energy than $c \ln^2 s$, where c is a constant and s is the square of the hadron-hadron center of mass system (cms).

In essence, FMS conclude that when all total cross section data for pp and $\bar{p}p$ between $5 \leq \sqrt{s} \leq 1800$ GeV are used—a total of 163 datum points—the measured total cross sections satisfactorily satisfy the relations

$$\sigma_{LE} = a_1 \left(\frac{s}{s_l} \right)^{-b_1} \pm a_2 \left(\frac{s}{s_l} \right)^{-b_2}, \quad (1)$$

$$\sigma_{HE} = \alpha + \beta \ln^\gamma \frac{s}{s_h}, \quad \gamma = 2, \quad (2)$$

$$\sigma_{\text{tot}} \equiv \sigma_{LE} + \sigma_{HE}, \quad (3)$$

where $a_1, a_2, b_1, b_2, \alpha, \beta, \gamma$ and s_h are real constants and $s_l = 1 \text{ GeV}^2$ and the + sign is for $\bar{p}p$ and the - sign is for pp collisions, i.e., they find that the Froissart bound is satisfied, but that is is violated ($\gamma > 2$) when *one* additional point at 7 TeV—the Totem [3] total cross section measurement of pp , $\sigma_{\text{tot}} = 98.3 \pm 0.2(\text{stat.}) \pm 2.8(\text{syst.})$ mb—is considered. As examples, see the $\gamma = 2$ result from Table 1, Direct Fit of FMS, and $\gamma = 2.104 \pm 0.027$ from Table 2, V1 of FMS. We will show that the statistical probability of the $\gamma = 2$ solution *with the inclusion* of the Totem result (Direct Fit model of Table 2, FMS) is *higher* than the statistical probability of the fit (Table 2, V1 model) that gave $\gamma > 2$. Thus, we find no statistical evidence for their claim.

Further, since they only include *one* additional high energy point at 7 TeV in their analysis, an alternate (and

in this case, perhaps more transparent) analysis method would have been to use the 163 pp and $\bar{p}p$ cross section datum points in the energy interval $5 \leq \sqrt{s} \leq 1800$ GeV to *predict* the 7 TeV total cross section. We will show that when we reanalyze the FMS results, the low energy fit for $\gamma = 2$ after including the errors of prediction (due to statistical errors in the parameters) *satisfactorily predicts* the 7 TeV Totem total cross section measurement.

We will also comment on the necessity for the simultaneous inclusion of the ρ data, the ratio of the real to the imaginary portion of the total cross section, together with the cross section data, i.e., a *global fit* of ρ and σ_{tot} , a statement alluded to (but *not* carried out) in the Appendix of FMS. Since all but one of the parameters is *common* to both ρ and σ , the simultaneous inclusion of the many ρ -values is important to an accurate fit, in order to minimize the (correlated) errors on the fitted parameters. We strongly disagree with the FMS comments 1 to 6 in their Section 2.2 concerning the ρ -values, in which they dismiss them as essentially useless, whereas in their Appendix, they give a rather cumbersome evaluation using their Variant 3 model, to *separately evaluate* ρ , and *not globally evaluate* it with the total cross sections, as demanded by analyticity.

Recently, eight measurements of pp cross sections have been made at energies higher than the Tevatron energy of 1800 GeV. At the LHC cms energy of 2.76 TeV, ALICE [4] has measured σ_{inel} , at the LHC cms energy of 7 TeV, ALICE [4], ATLAS [5], CMS [6] and TOTEM [3] have measured σ_{inel} ; σ_{tot} has been measured by TOTEM [3]. Most recently, the Pierre Auger Observatory has published pp cross sections for σ_{inel} and σ_{tot} at 57 TeV [7], using cosmic ray measurements of extended air showers to measure $\sigma_{\text{p-air}}$. Most likely, this is effectively the highest energy reach that one will ever have experimentally.

Finally, using these ultra-high energy measurements, we will summarize a very recent analysis of Block and Halzen [8] that shows that the proton asymptotically be-

comes a *black disk*, whose total cross section asymptotically varies with energy as a *saturated* Froissart bound, i.e., as $\ln^2 s$, and whose asymptotic ratio of inelastic to total cross section is $1/2$, that of the black disk. This result, using *all available* high energy data, including inelastic cross sections, clearly contradicts the conclusions of FMS.

Statistical Probabilities—For a χ^2 fit, the goodness-of-fit criterion for a given model is normally taken as $P(\chi_0^2; \nu)$, the integral of the probability distribution in χ^2 for ν degrees of freedom, integrated from the observed minimum χ_0^2 to infinity; it is $P(\chi_0^2; \nu)$ that allows us to statistically distinguish between models. From Table 1 of FMS, we concentrate on the Direct Fit (DF₁) and V1 models, which give $\chi_0^2 = 145.236$, $\nu = 156$, yielding $P_{DF_1} = 0.721$, whereas for V1, we have $\chi_0^2 = 145.235$, $\nu = 155$, yielding $P_{V_1} = 0.701$. Thus, even though FMS relaxed the input restriction that $\gamma = 2$ and allowed it to be fit by the data, we get the somewhat strange result that FMS have a *better, somewhat more reliable* fit when they fix the value of γ at 2, the Froissart bound limit, than when they allow it to float, suggesting perhaps that the *true* minimum χ^2 was not achieved in their minimization process. In any event, FMS concluded that the value $\gamma = 2$ was correct for the energy interval $5 \leq \sqrt{s} \leq 1800$ GeV.

Next, we calculate the goodness-of-fit probabilities for the Direct Fit and V1 models from Table 2, which now includes *one additional point*, the Totem point at 7 TeV. For the Direct Fit model (DF₂), we find $\chi_0^2 = 146.01$, $\nu = 157$, giving $P_{DF_2} = 0.725$; this is effectively *identical* to the comparable value obtained ($P_{DF_1} = 0.721$) not using the Totem point. Thus, if $\gamma = 2$ is satisfactory for the low energy data, it appears to be exactly the same level of confidence when we include the Totem point. Finally, we calculate from Table 2 the high energy version of the V1 model (V1₂), i.e., $\chi_0^2 = 145.86$, $\nu = 156$, giving $P_{V1_2} = 0.709$, a probability *smaller* than that of the Direct Fit model (DF₂), i.e., $P_{DF_2} = 0.725$. Again, this result is somewhat strange, since the logarithmic power γ was left adjustable in the V1₂ model.

Completely analogous results were found when comparing the V4 and V5 models from Table 3. We obtain $P_{V4_1} = 0.616$ for fixed $\gamma = 2$ and $P_{V5_1} = 0.595$ when FMS let γ float for the low energy data—again, it is very strange that letting γ be fit by the data gave a lower probability than fixing γ to be 2.

To illustrate this anomaly, we recall to the reader that the difference between the V4₁ and the Direct Fit (DF₁) models was that in the V4 model, the Regge powers b_1 and b_2 were fixed at $1/2$, whereas they were allowed to vary in the Direct Fit model, *raising* the probability from $P_{V4} = 0.616$ to $P_{V6} = 0.721$, as expected—the *exact opposite* of the V4 to V5 effect, where the logarithmic power γ was varied from 2. Clearly, we question their minimization program, or their use of it.

Thus, we conclude that there is no statistical evidence given in FMS that supports the conclusion that $\gamma > 2$, and thus, no basis for concluding that the Froissart bound is violated.

Prediction of the 7 TeV total pp cross section—Since Table 1 of FMS does not contain the Totem point, its data could have been used to make predictions of the total cross section at 7 TeV to compare with the Totem value, since it uses only lower energy data, although the FMS paper has not explicitly made any predictions. However, their plots of their results in Tables 1 and 3 allow us to do so, visually. Inspection of the curve for the V4 model in Fig. 5 of FMS (the dash-dotted curve) shows that the central value of the 7 TeV prediction (from the data using *only* the lower energies, labeled $\sqrt{s}_{\max} = 1.8$ TeV) goes slightly inside the lower error bar of the plotted Totem result. To obtain their 7 TeV cross section prediction, together with its error, from their V4 model of Table 3 using their parameters in a standard error evaluation, we find $\sigma_{\text{tot}} = 96.2 \pm 4.5$ mb, which is in excellent agreement with the experimental value of 98.1 ± 2.3 found by Totem. We see indeed that the Totem value is well predicted using $\gamma = 2$, with the FMS numbers that they themselves calculated.

Similar conclusions may be drawn from the Direct Fit model of Table 1. Using the Direct Fit model parameters of FMS's Table 1, we numerically calculate that the DF model predicts 95.4 ± 3.7 mb when *only* the 1σ diagonal error due to the coefficient β is taken into account; it becomes 95.4 ± 8.8 when their diagonal error due to s_h is included), so that their DF model prediction is also in good agreement with the Totem cross section, 98.1 ± 2.3 mb.

As in the preceding Section, we find that the FMS $\gamma = 2$ fits at low energy, after allowing for errors in the predictions due to the statistical errors in the fitting parameters, successfully predict the Totem total cross section at 7 TeV, thus negating the necessity for considering a violation of the Froissart bound. In simpler words, the FMS fits are consistent with a saturated Froissart bound when the Totem point is included.

Additional experimental evidence for a saturated Froissart bound—Block and Halzen [8] (BH) have recently shown that the proton asymptotically becomes a black disk as $s \rightarrow \infty$, using analyticity constraints that anchor their fit at low energy to predict ultra-high energy experimental data at the LHC at 7 TeV, as well as the Pierre Auger Observatory [7] results at 57 TeV. The BH model parameterizes the even and odd (under crossing) total cross sections and ρ -values and fits 4 experimental quantities, the 2 total cross sections $\sigma_{\bar{p}p}(\nu)$, $\sigma_{pp}(\nu)$ and the 2 ρ -values, $\rho_{\bar{p}p}(\nu)$ and $\rho_{pp}(\nu)$, to the high energy analytic (complex) amplitude parameterizations [9], which guarantee analyticity and are much simpler to compute than derivative dispersion relations. Using ν as the laboratory energy and denoting m as the proton mass, they

find that

$$\sigma^0(\nu) \equiv \beta_{\mathcal{P}'} \left(\frac{\nu}{m}\right)^{\mu-1} + c_0 + c_1 \ln\left(\frac{\nu}{m}\right) + c_2 \ln^2\left(\frac{\nu}{m}\right), \quad (4)$$

$$\sigma^\pm(\nu) = \sigma^0(\nu) \pm \delta \left(\frac{\nu}{m}\right)^{\alpha-1}, \quad (5)$$

$$\rho^\pm(\nu) = \frac{1}{\sigma^\pm(\nu)} \left\{ \frac{\pi}{2} c_1 + c_2 \pi \ln\left(\frac{\nu}{m}\right) - \beta_{\mathcal{P}'} \cot\left(\frac{\pi\mu}{2}\right) \left(\frac{\nu}{m}\right)^{\mu-1} + \frac{4\pi}{\nu} f_+(0) \pm \delta \tan\left(\frac{\pi\alpha}{2}\right) \left(\frac{\nu}{m}\right)^{\alpha-1} \right\}, \quad (6)$$

using the upper sign for pp and the lower sign for $\bar{p}p$; $\delta, \alpha, \beta_{\mathcal{P}'}, \mu, c_0, c_1, c_2$ and $f_+(0)$ are real constants, with $f_+(0)$ being the singly subtracted dispersion relation constant. $\sigma^0(\nu)$, the even (under crossing) amplitude cross section of Eq. (4) effectively becomes

$$\sigma^0(s) = c_0 + c_1 \ln\left(\frac{s}{2m^2}\right) + c_2 \ln^2\left(\frac{s}{2m^2}\right), \quad (7)$$

so that asymptotically, $\sigma^0 \rightarrow \ln^2 s$. Thus, the high energy functional form used by FMS, Eq. (2), when $\gamma = 2$, is completely equivalent to the functional form of the above Eq. (7). In other word, BH replace the 3 FMS parameters α, β and s_h by the 3 linear parameters c_0, c_1 and c_2 . Thus, the BH fit uses approximately the same physical assumptions as the V4 model in Table 3 of FMS, fitting data for cms energies $\sqrt{s} \leq 1800$ GeV.

The results [10] of a *global* fit to both $\bar{p}p$ and pp ρ -values and total cross sections in the energy range $6 \leq \sqrt{s} \leq 1800$ GeV, with 187 datum points and *only* 5 free parameters, δ, α, c_1, c_2 and $f_+(0)$, is shown in Fig. 1. As seen from Eq. (6), $\rho \rightarrow 0$ as $s \rightarrow \infty$, which is a re-

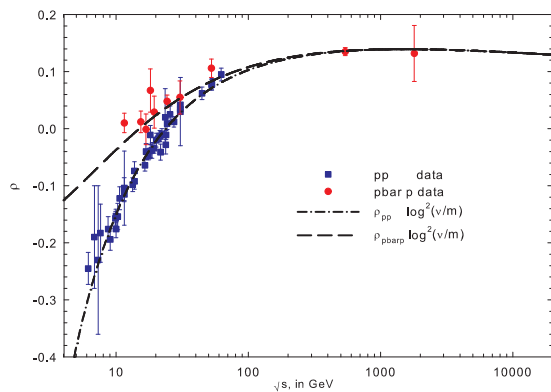


FIG. 1: Froissart-bounded analytic amplitude fits to ρ , the ratio of the real to the imaginary portion of the forward scattering amplitude, vs. \sqrt{s} , the cms energy in GeV, taken from BH [10]. The $\bar{p}p$ data used in the fit are the (red) circles and the pp data are the (blue) squares.

quirement for a black disk at infinity. However, the tiny change in ρ from 0.135 at 1800 GeV to 0.132 at 14000 GeV implies that we are nowhere near asymptopia, where $\rho = 0$.

The fits for the pp and $\bar{p}p$ total cross sections, that use only 4 of the *same* parameters that were used for the ρ -value fit of Fig. 1, are shown in Fig. 2. The

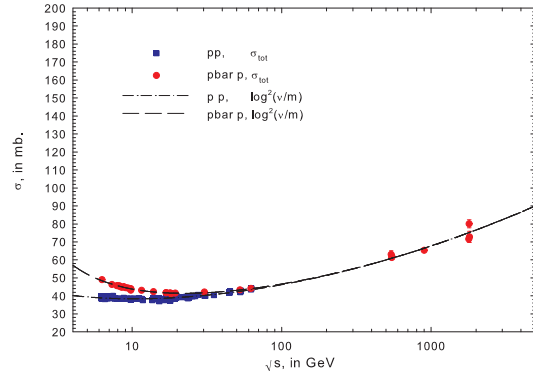


FIG. 2: Froissart-bounded analytic amplitude fits to the total cross section, σ_{tot} , in mb, for $\bar{p}p$ (dashed curve) and pp (dot-dashed curve) from Eq. (5), vs. \sqrt{s} , the cms energy in GeV, taken from BH [10]. The $\bar{p}p$ data used in the fit are the (red) circles and the pp data are the (blue) squares. The fitted data were anchored by values of $\sigma_{\text{tot}}^{\bar{p}p}$ and σ_{tot}^{pp} , together with the energy derivatives $d\sigma_{\text{tot}}^{\bar{p}p}/d\nu$ and $d\sigma_{\text{tot}}^{pp}/d\nu$ at 6 GeV using FESR, as described in Ref. [10]. We note that their ultra-high energy total cross section predictions that are made from their analytic amplitude fit use *only* total cross section data that are in the lower energy range $6 \leq \sqrt{s} \leq 1800$ GeV.

dominant $\ln^2 s$ term in the total cross section σ^0 (see Eq. (7)) saturates the Froissart bound [2]; thus it controls the ultra-high energy behavior of the total cross sections.

A very important role in fixing the overall fit is played by Finite Energy Sum Rules (FESR) [11, 12] anchoring the fit at the low energy end, taken to be $\sqrt{s} = 6$ GeV. The FESR allow BH [10] to fix the fit to both $\sigma_{\text{tot}}^{\bar{p}p}$ and σ_{tot}^{pp} , together with their two energy derivatives $d\sigma_{\text{tot}}^{\bar{p}p}/d\nu$ and $d\sigma_{\text{tot}}^{pp}/d\nu$, at the low end, $\sqrt{s} = 6$ GeV, by using the many precise low energy total cross section measurements between \sqrt{s} of 4 and 6 GeV. These FESR constraints then can be used to evaluate directly the values of c_0 and $\beta_{\mathcal{P}'}$, two of the four parameters needed to determine σ^0 , the even high energy total cross section of Eq. (4). These fixed values of c_0 and $\beta_{\mathcal{P}'}$, together with the 2 *globally fitted* values of c_1 and c_2 required for $\sigma^0(\nu)$ (obtained from fitting *simultaneously* the high energy total cross section and ρ measurements in the energy region $6 \leq \sqrt{s} \leq 1800$ GeV), are listed in Table I. We remind the reader that only data in the energy region $6 \leq \sqrt{s} \leq 1800$ GeV are used in this global fit (together with the prolific and accurate 4 to 6 GeV total cross section data used for the 6 GeV low energy ‘anchor points’). We note that c_2 , the coefficient of $\ln^2(s)$, is well-determined, having a

statistical accuracy of $\sim 2\%$. Thus, we see from Fig. 2 that the experimental data show that a saturated Froissart bound model is accurately satisfied for σ_{tot} , the total cross sections for both $\bar{p}p$ and for pp in the energy interval $6 \leq \sqrt{s} \leq 1800$ GeV; this accuracy of prediction mainly results from the use of the FESR constraints on the high energy analytic amplitude fit [11, 12]. Ultra-high energy total cross sections, for which there are no distinction between $\bar{p}p$ and pp interactions—both being given by σ^0 —are now accurately predicted. For example, we obtain values for the total pp cross section of $\sigma^0 = 95.4 \pm 1.1$ mb at 7 TeV [13] and 134.8 ± 1.5 mb at 57 TeV [14], where the $\pm 1\sigma$ errors are calculated from the (correlated) errors of their fit parameters c_1 and c_2 . The (black) upper curves in Fig. 3 are plots of these BH [8] predictions for the total cross section σ^0 vs. \sqrt{s} , with the solid curve being the central value and the dashed curves the $\pm 1\sigma$ error curves.

TABLE I: Values of the parameters, in mb, needed for the even amplitude total cross section, $\sigma^0(\nu)$ of Eq. (4), taken from Ref. [10].

$c_0=37.32$ mb,	$\beta_{\mathcal{P}'}=37.10$ mb
$c_1=-1.440 \pm 0.070$ mb,	$c_2=0.2817 \pm 0.0064$ mb,

The inelastic cross section, σ_{inel}^0 , is determined by numerically multiplying the ratio of the inelastic to total cross section with the fitted total cross section σ^0 . The ratio of inelastic to total cross section was determined from an eikonal model, called the ‘Aspen’ model; for details see Ref. [15] and Ref. [16].

Block and Halzen [16] found that

$$\sigma_{\text{inel}}^0(\nu) = 62.59 \left(\frac{\nu}{m}\right)^{-0.5} + 24.09 + 0.1604 \ln\left(\frac{\nu}{m}\right) + 0.1433 \ln^2\left(\frac{\nu}{m}\right) \text{ mb}, \quad (8)$$

valid in the energy domain, $\sqrt{s} \geq 100$ GeV.

The lower (red) plots of Fig. 3 are the BH [8] predictions (Eq. (8)) for high energy *inelastic* cross sections σ_{inel} , as a function of \sqrt{s} . The solid (red) plot is the central value and the error bands corresponding to $\pm 1\sigma$ are the lower dashed (red) curves. All of the existing inelastic cross section measurements for $\bar{p}p$, as well as the eight new ultra-high pp measurements, are shown. The agreement with experiment is excellent over the entire energy scale. In particular, the agreement with the new highest energy (57 TeV) experimental measurements of both σ_{tot} and σ_{inel} is striking. Since *none* of the experimental datum points in Fig. 3 were used in making these predictions, it is clear that the $\ln^2 s$ predictions for σ_{inel} and σ_{tot} are strongly supported by the existing ultra-high energy measurements.

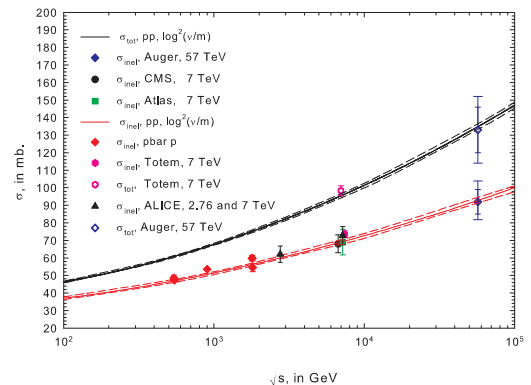


FIG. 3: Predictions for σ_{tot} and σ_{inel} , in mb, vs. \sqrt{s} , in GeV, for $\bar{p}p$ and pp , taken from Block and Halzen [8]. For σ_{tot} , they have compared their predictions with recent pp TOTEM data at 7 TeV and Auger data at 57 TeV, while for σ_{inel} , they have compared their results with 2.76 TeV pp data from ALICE, 7 TeV pp data from ALICE, ATLAS, CMS and Totem, as well as with the 57 TeV pp inelastic cross section. The upper solid (black) curve is the central-value prediction for σ_{tot} and the lower solid (red) curve is the central-value prediction for σ_{inel} . The dotted curves are the errors ($\pm 1\sigma$) in their predictions, due to the correlated errors of the fitting parameters.

Finally, BH [16] determined the ratio of $\sigma_{\text{inel}}(s)/\sigma_{\text{tot}}(s)$ as $s \rightarrow \infty$, given by the ratio of the $\ln^2 s$ coefficients in σ_{inel}^0 and σ^0 , respectively, i.e.,

$$\frac{\sigma_{\text{inel}}}{\sigma_{\text{tot}}} \rightarrow \frac{c_2^{\text{inel}}}{c_2} = \frac{0.1433}{0.2817} = 0.509 \pm 0.021, \quad \text{as } s \rightarrow \infty, \quad (9)$$

that is well within error of the expected value of $\frac{1}{2}$ that is appropriate for a black disk at infinity.

Conclusions—We find that:

1. there is no sound statistical evidence put forth by FMS [1] for their conclusion that the Froissart bound is exceeded. Their models with $\ln^2 s$ that only use lower energy cross sections actually *predict* the Totem total pp cross section reasonably well.
2. *both* the measured total pp cross sections and the inelastic cross sections are fit up to $\sqrt{s} = 57$ TeV by a saturated Froissart-bounded $\ln^2 s$ behavior that is associated with a black disk.
3. the forward scattering amplitude is pure imaginary as $s \rightarrow \infty$, as is required for a black disk.
4. the ratio of $\sigma_{\text{inel}}/\sigma_{\text{tot}} \rightarrow 0.509 \pm 0.021$, as $s \rightarrow \infty$, compatible with the black disk value of 0.5.

Thus, we conclude that existing experimental evidence strongly supports the conclusion that the proton becomes a black disk at infinity, whose total cross section goes as $\ln^2 s$ as $s \rightarrow \infty$.

Acknowledgments—In part, F. H. is supported by the National Science Foundation Grant No. OPP-0236449, by the DOE grant DE-FG02-95ER40896 and by the University of Wisconsin Alumni Research Foundation. M. M. B. thanks the Aspen Center for Physics, supported in part by NSF Grant No. 1066293, for its hospitality during this work.

-
- [1] The preceding paper in the Braz. J. Phys., Vol. 42 (2012) by D. A. Fagundes, M. J. Menon and P. V. R. G. Silva, arXiv:1112.4704 (2012).
- [2] M. Froissart, Phys. Rev. **123**, 1053, 1961.
- [3] Totem Collaboration, EPL **96**, 21002 (2011).
- [4] M. Gagliandi for the ALICE collaboration, indico.cern.ch/getFile.py/access?contribId=0&sessionId=0&resId=0&materialId=slides&confId=140054 (2011).
- [5] Atlas Collaboration, Nature Comm., **2**, article number 463, DOI 1038/ncomms1472 (2011).
- [6] CMS Collaboration, CERN Document Server, <http://cdsweb.cern.ch/record/1373466?ln=en>, August 27, 2011.
- [7] Pierre Auger Collaboration, Phys. Rev. Lett. **109**, 062002 (2012).
- [8] M. M. Block and F. Halzen, Phys. Rev. D **86**, 051504 (2012).
- [9] M. M. Block and R. H. Cahn, Rev. Mod. Phys. **57**, 563 (1985).
- [10] M. M. Block and F. Halzen, Phys. Rev. D **72**, 036006, (2005); **73**, 054022 (2006).
- [11] M. M. Block, Eur. Phys J. C **47**, 697, 2006.
- [12] M. M. Block, Phys. Rep. **436**, 71 (2006).
- [13] M. M. Block and F. Halzen, Phys. Rev. D **83**, 077901 (2011).
- [14] M. M. Block, Phys. Rev. D **84**, 09150 (2011).
- [15] M. M. Block, E. Gregores, F. Halzen and G. Pancheri, Phys. Rev D **60**, 054024 (1999).
- [16] M. M. Block and F. Halzen, Phys. Rev. Lett. **107**, 212002 (2011).